ISSN 1070-3632, Russian Journal of General Chemistry, 2021, Vol. 91, No. 3, pp. 546–553. © Pleiades Publishing, Ltd., 2021.
Russian Text © The Author(s), 2019, published in Rossiiskii Khimicheskii Zhurnal, 2019, Vol. 63, No. 2, pp. 17–25.

Structure and Properties of Biopolymeric Fibrous Materials Based on Polyhydroxybutyrate–Metalloporphyrin Complexes

A. A. Ol'khov[a,b,c,*], P. M. Tyubaeva[a,c], Yu. N. Zernova[b], A. S. Kurnosov[c], S. G. Karpova[c], and A. L. Iordanskii[b]

[a] *Plekhanov Russian University of Economics, Moscow, 117997 Russia*
[b] *Semenov Institute of Chemical Physics, Russian Academy of Sciences, Moscow, 119991 Russia*
[c] *Emanuel Institute of Biochemical Physics, Russian Academy of Sciences, Moscow, 119334 Russia*
**e-mail: aolkhov72@yandex.ru*

Received January 1, 2019; revised January 10, 2019; accepted January 10, 2019

Abstract—Ultrathin fibrous materials based on natural bacterial polymer polyhydroxybutyrate (PHB) were prepared by the electrospinning method. Using scanning electron and optical microscopy techniques the macrophysical characteristics of the fibrous layer were determined and classified. The physicomechanical characteristics of the resultant materials and their changes caused by ozonation were determined as well. Structure formation in the ultrathin polyhydroxybutyrate fibers containing low antibacterial concentrations was studied. The effect of low concentrations of zinc tetraphenylporphyrin and iron(III) chloroteteraphenylporphyrin complexes on the structure of polyhydroxybutyrate-based ultrathin fibers was elucidated. Techniques used in the study were X-ray diffraction analysis, ESR spin probe method, differential scanning calorimetry, and optical and electron scanning microscopy. It was shown that addition of the metal porphyrin complexes caused changes in the degree of crystallinity and in the crystallite size of the PHB fibers, while the proportion of dense domains in the amorphous phase of the polymer fiber increased.

Keywords: ultrafine fibers, electrospinning, polyhydroxybutyrate, ozonation, physicomechanical characteristics, structure, metalloporphyrin complexes

DOI: 10.1134/S1070363221030245

INTRODUCTION

Development and study of biopolymer-based nonwoven fibrous materials intended for medical application attract much practical interest today [1]. One of the most promising methods for producing nonwoven materials with large surface area is electrospinning (ES). The ES method is based on pulling the polymer solution as a thin viscous jet in a field of mechanical and electrostatic forces, followed by forming a fiber with the diameter ranging from tens to thousands of nanometers.

Study of electrospun nonwoven materials allowed summarizing several key factors governing the structural organization in the material at the macrostructure [packing and relative positions of the nonwoven fabric elements (fibers)] [2] and the microstructure (orientation of the polymer molecules in a material) [3] levels.

Macrophysical characteristics of fibrous materials are essential for describing in detail the features of the fibrous layer and establishing the relationship between the fiber formation process and a number of properties determined by the parameters of both the individual fibers and the entire material. Among the basic characteristics of the structural organization in a fibrous material of critical importance are the following: the relative density of the fibers of the structure, fiber orientation index, materials intensity, average surface density, and average fiber diameter.

These characteristics have a sizable effect on the physicomechanical properties of fibrous materials. The overwhelming majority of electrospun polymer materials consist of sufficiently dry fibers that are practically incapable of reversible elastic deformations. One of the most important criteria for assessing the mechanical

properties of such materials is the behavior under uniaxial tension test conditions.

In respect to medicinal products and materials, of great research interest is how they are influenced by ozonation, which is one of the most effective methods of their sterilization and disinfection [4]. Particularly important is assessment of changes in the mechanical properties of the material, caused by ozonation. Polymer matrices with bactericidal properties can be prepared with the use of various types of chemical compounds able to inhibit the growth of pathogenic microorganisms. Among new biologically active substances, mention should be made of metalloporphyrin complexes acting as homogeneous catalysts in autooxidation of a number of biogenic substances. Intermediates generated during this process are reactive oxygen species such as superoxide anion radical, peroxide and hydroxyl radicals, and hydrogen peroxide with known cytostatic activity. Oxidation reactions involving these radicals and radical ions cause bactericidal effect.

Highly porous polymeric carriers of biologically active substances find extensive biological and medicinal application as prolonged-action matrices, cellular engineering scaffolds, antibacterial therapeutic agents, controlled drug release matrices, etc. [5]. Antibacterial polymeric systems can be developed using porphyrin complexes with various metals [6]. High effectiveness is demonstrated by zinc and iron tetraphenylporphyrin complexes which cause UV irradiation-induced conversion of molecular oxygen into reactive species exerting a strong oxidative effect on bacterial microflora. One of the most economically and technologically effective methods of creating film-type matrices based on nanosized and ultrathin fibers is electrostatic drawing of fibers from polymer solutions and melts [7]. Numerous studies have shown that the morphology of the polymer fibers significantly affects the set of physicomechanical and diffusion properties and the biodegradation kinetics [8]. The supramolecular structure of the fibers is influenced not only by the molecular characteristics of the polymer and the process parameters of electrospinning such as polymer concentration, temperature, etc., but also by additions of substances of different chemical nature to the spinning solution [9, 10]. In view of the above-said, obtaining electrospun fibers with target morphology is an urgent and practically significant task.

The aim of this study was to examine the influence exerted by zinc tetraphenylporphyrin (ZnTPP) and iron(III) chlorotetraphenylporphyrin [Fe(III)ClTPP)] complexes on the supramolecular structure of electrospun ultrathin poly-3-hydroxybutyrate (PHB) fibers.

EXPERIMENTAL

In our study we used natural biodegradable polymer poly-3-hydroxybutyrate of the 16F series from Biomer (FRG), produced by bacterial fermentation. The viscosity-average molecular weight of PHB was 2.06×10^5. The fibers were obtained by the ES method using a single-capillary electrospinning laboratory unit at a capillary diameter of 0.1 mm, electric current voltage of 12 kV, electrode gap of 18 cm, and solution conductivity of 10 μS/cm. For producing fibrous matrices with antiseptic properties served ZnTPP and Fe(III)ClTPP complexes [11–13]. Electrospinning solutions were prepared in chloroform at 50°C using an automatic magnetic stirrer. The PHB concentration in the solution was 7 wt %, and the content of the complexes in the electrospinning solution, 1, 3, or 5 wt % of the PHB mass.

The electrospinning conditions exert a great influence on the nature and structure of fiber distribution in the material. Importantly, the structure of the material as a whole is irregular, with randomly oriented fibers. In this study, fiber distribution was examined by a set of methods of optical and scanning electron microscopy.

Mechanical properties were evaluated by the uniaxial stretching method on a DEVOTRANS (Turkey) tensile testing machine in accordance with GOST (State Standard) R 53226-2008 "Nonwoven fabrics: Methods for strength determination."

Ozonation of the materials was carried out with the use of ozonizer in the laboratory of the Emanuel Institute of Biochemical Physics, Russian Academy of Sciences. Ozone was generated from oxygen by electric discharge process, where an increase in voltage led to that in the gas concentration. The experiment was carried out at the working ozone concentration of 5.5×10^{-5} M. The absorbed ozone volume was estimated using an SF-46 Lomo spectrophotometer via measuring the optical density of the medium at a wavelength of 254 nm. The gas flow rate was 101.8 mL/min, and the time of ozonation of the material samples ranged from 3 to 5 min.

The X-ray diffraction analysis of the PHB fibers was carried out on a diffractometer with a linear position-sensitive (coordinate) detector [8, 9] (CuK_α radiation, sample-detector distance 110 mm, measurements in the region of small and large scattering angles using

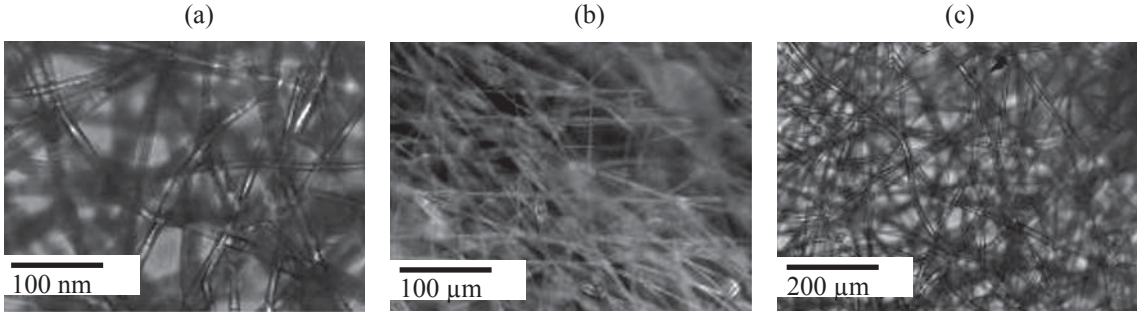

Fig. 1. Micrographs of the PHB-based nonwoven fibrous material: (a) medium, (b) regular, and (c) random fiber distribution (optical microscopy method).

transmission geometry) and on an HZG4 diffractometer (Freiberger Präzisionsmechanik, FRG) with a diffracted beam graphite monochromator in the Bragg-Brentano reflection geometry (CuK_α radiation, measurements in the region of large scattering angles using reflection geometry). X-band ESR spectra were recorded on an EPR-V automated spectrometer (Russia). TEMPO stable nitroxyl radical was used as a probe. The radical was introduced into the fibers from the gas phase at a temperature of 50°C; its concentration in the polymer did not exceed 10^{-3} M. The geometry of the fibrous materials was examined with a Micromed Polar 3 ToupCam 5.1 MP (China) optical microscope in reflected light at magnification 200x and with a Hitachi TM-3000 scanning electron microscope (Japan) (at an accelerating voltage of 20 kV; a 100–200 Å thick gold layer was sprayed on the surface of a nonwoven fibrous material sample). The DSC study of the samples was conducted on a Netzsch DSC 204 F1 instrument in an argon atmosphere at a heating rate of 10°C/min.

RESULTS AND DISCUSSION

In this study, three main types of fiber distribution were identified: regular, medium, and random. Figure 1 shows the microphotographs of different types of fiber packing in the material, which were obtained with a Polar 3 Mikromed (Russia) polarizing transmission microscope. Table 1 lists a number of macrophysical characteristics that are distinctive to these materials and characterize the morphology of their fibrous layer.

The relative density of the structure corresponds to the proportion of fiber-free volume of the material and is related to the packing density of the fibers in the porous layer of the material; for electrospun materials it typically ranges from 80 to 98%. The specific mass of the fibers in the material is described through the surface density of the layer. The fiber orientation index characterizes the direction and specific features of their crimp per unit area for a specified thickness of the fibrous layer. Combined, these characteristics enable assessment of the efficiency of the ES process and provide a means to prevent many fiber surface defects, as well as elastic shrinkage and adhesion of the fibers during the jet curing on the electrode, and also to influence the formation of the functional, in particular physicomechanical properties.

An important parameter for assessing the uniformity and degree of variation of the characteristics of individual elements in the fibrous material structure is the fiber diameter distribution. In this study, it was evaluated from the per unit area numbers and average diameters of fibers (400×300 μm) as derived from a series of micrographs obtained by direct methods of optical and scanning microscopy (Fig. 2).

Table 1. Structural parameters of the nonwoven fibrous materials

Main structural parameters	Fiber distribution type		
	regular	medium	random
Fiber orientation index φ, rel. units	0.74	0.67	0.36
Surface density, mg/m^2	36	26	16
Average fiber diameter d, μm	8.6	8.1	9.2
Relative density γ, %	98	89	84

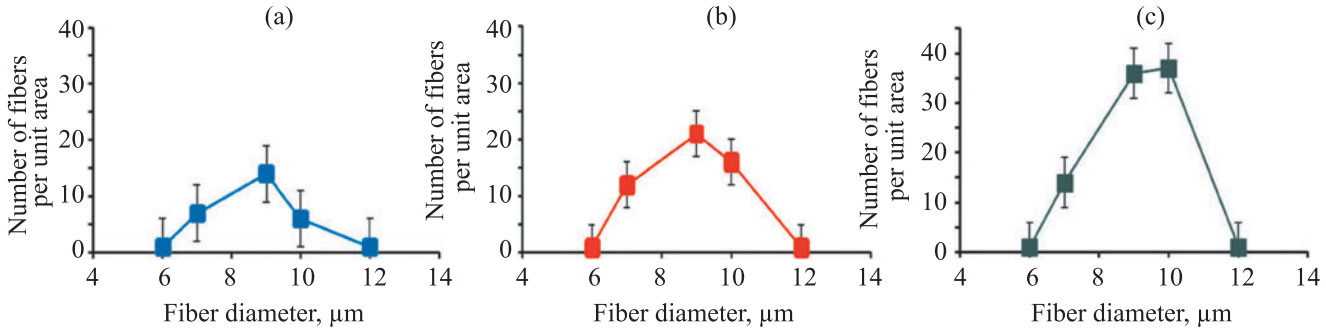

Fig. 2. Fiber diameter distribution for the PHB-based nonwoven fibrous material: (a) medium, (b) regular, and (c) random fiber distribution.

Study of the structural features of the materials of interest showed that, with a decrease in the average fiber diameter, the fiber twist, crimp, and packing density tend to increase. This improved mechanical characteristics such as breaking length of the material, while having little effect on the elongation at break.

Taken together, the above-listed characteristics of the macrostructure of the nonwoven materials allow fairly accurately assessing the average interfiber distance and the fiber packing density, type, and average diameters, as well as deviations from average values, variation per unit area, and presence of defects. The irregularity of the materials obtained in this study did not exceed 10%. Depending on fiber distribution, the breaking load ranged from 1.4 to 2.2 N, and the relative deformation, from 1.1 to 4%.

Considering the intended medicinal application of the materials studied, we chose the regular distribution as the best suited to evaluating the mechanical properties of the PHB-based nonwoven fibrous fabrics and their changes caused by sterilization with ozone. The volume of the gas absorbed during ozonation, depending on the type of the fiber distribution in the material structure, was estimated at 300–330, 400–440, and 450–480 mol/m^2 for regular, medium, and random distribution types, respectively.

A series of experiments showed that, under the influence of ozone, the breaking load of the PHB-based nonwoven fibrous materials displayed an approximately twofold increase (see Table 2). Moreover, mechanical properties such as the modulus of elasticity, relative deformation, and maximum elongation at break noticeably increased as well.

Improvement of the strength properties of the material, caused by ozonation, may be accounted for primarily by oxidation of the PHB macromolecules. An increase in the number of functional groups, characteristic of the ozone oxidation mechanism, causes an increase in polarity of the molecules via accumulation of oxygen-containing functional groups, thereby improving the strength characteristics of the material. Another possible reason for enhancement of the strength properties consists in increases in the degree of crystallinity and in the size of the crystalline PHB formations in the fiber, caused by ozonation.

Further, we considered some aspects of formation of the supramolecular structure of the PHB fibers upon addition of low concentrations of antibacterial agents such as tetraphenylporphyrin metallocomplexes.

Adding ZnTPP complex to the PHB solution caused significant changes in the fiber morphology. The original PHB fiber (inset in Fig. 3a) exhibited alternation of cylindrical and spindle-like segments. The presence of thickened segments in the fiber structure is attributable to low electrical conductivity and low surface tension of the polymer spinning solution. The average diameter of the cylindrical segments of the fiber was 1–3 μm, and the spindle-like segments had a maximum diameter of ~10 μm and a length of 20–30 μm. Adding 1–5% ZnTPP to the PHB solution caused complete disappearance of the spindle-like segments in the fiber structure (inset in

Table 2. Physicomechanical properties of the nonwoven fibrous materials

Sample	Breaking load, N	Modulus of elasticity, MPa	Relative deformation,%	Displacement, mm
PHB	1.7	39.8	3.4	1.4
PHB after ozonation	3.5	58.8	7.6	2.3

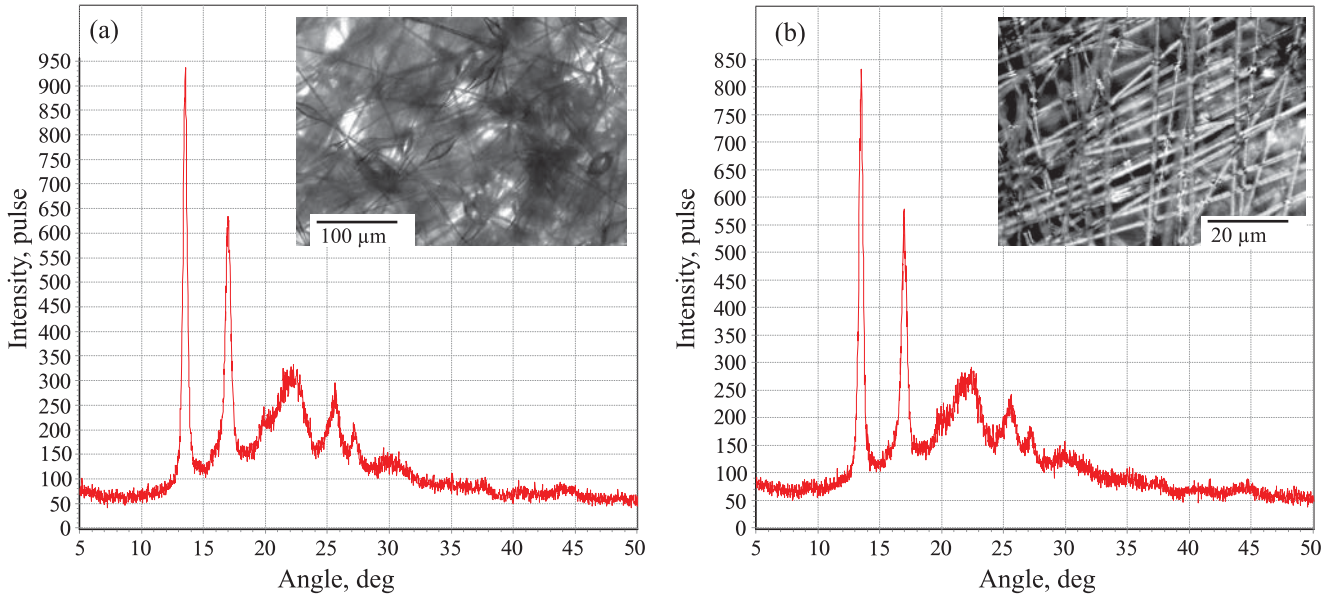

Fig. 3. X-ray diffraction patterns of the PHB fibers (recorded in reflection Bragg-Brentano geometry): (a) 0% ZnTPP and (b) 5% ZnTPP.

Fig. 3b). The thickened segments could disappear because of an increase in electrical conductivity of the spinning solutions upon adding polar ZnTPP complexes which moreover exhibit paramagnetic properties. Increase in electrical conductivity caused more intensive drawing of a solution droplet in the field of action of electrostatic force, which led to equalization of thickness of the fibers. With increase in the ZnTPP concentration in the spinning solution its viscosity grew due to the intermolecular interaction of the polar molecules of the complex with the polar groups of PHB. The surface tension of the solution increased, and the primary solution jet did not split. The diameter of the resultant fibers of PHB containing 3–5% ZnTPP complex was estimated at 3–4 μm.

Figure 3 presents the X-ray diffraction patterns recorded in the region of large scattering angles for the PHB fibers containing 0 and 5% ZnTPP. .

The position of peaks (lines) in these diffraction patterns corresponds to the crystal lattice of PHB with an orthorhombic unit cell (a = 0.576 nm, b = 1.320 nm, c = 0.596 nm). According to the optical microscopy data, the PHB fibers lie predominantly in the material plane, so no noticeable preferred orientation is manifested by the crystallites in the fibers proper. It was found that, upon adding 1, 3, and 5% ZnTPP, the degree of crystallinity of the PHB fibers remained unchanged at 45–53%. The calculation of the average crystallite sizes was based on (020), (101) and (111) diffraction peaks obtained using Bragg-Brentano geometry for all the samples. It is seen that the crystallite sizes are identical for PHB and PHB containing 5% ZnTPP, specifically, L_{020} = 26–27 nm in the crystallite plane, and 5–6 nm in the L_{101} and L_{111} planes.

The small-angle X-ray diffraction patterns of the fibers of PHB containing 0, 1, 3, and 5% ZnTPP exhibit a peak corresponding to the long period $D = (S_{max})^{-1}$ of 5.4–5.7 nm for all the samples studied. Small-angle X-ray scattering analysis by the Tsvankin method revealed the PHB crystallite thickness of ~4 nm for all the samples. The latter data agree very well with the crystallite thicknesses derived from the breadth of the diffraction lines in the region of large scattering angles.

The structure of the amorphous domains is substantially determined by the proportion of the crystalline and paracrystalline formations. Small ZnTPP additions cause the proportion of paracrystalline structures in PHB to increase, thereby changing the structural and dynamic properties of the amorphous domains. The molecular dynamics of these domains can be studied most conveniently by the ESR method using stable radicals. The ESR spectra of TEMPO radical in the PHB matrix exhibit a complex shape, being a superposition of two spectra corresponding to two populations of radicals with different correlation times τ_1 and τ_2, of which τ_1 characterizes the molecular mobility in denser and τ_2, in looser amorphous domains (Fig. 4).

With increasing porphyrin concentration in the PHB fibers the proportion of dense domains exhibited nearly sixfold increase. The correlation time in the dense domains also increased, with τ changing most dramatically upon adding 1% porphyrin to the fiber; further increase in the ZnTPP concentration caused a smoother increase in the correlation time.

In this study, the correlation time τ_2 was calculated from the ESR spectra as $5\times10^{-11} < \tau_2 < 10^{-9}$ s. The dependence of τ_2 on the ZnTPP concentration is nonlinear. We presumed that the increase in the correlation time τ in the mixed compositions was due to deceleration of the molecular mobility because of amorphous phase condensation. An increase in the proportion of paracrystalline structures is commonly paralleled by that in the proportion of straightened chains in the amorphous interlayer and, thereby, by deceleration of the molecular mobility. Such changes in the amorphous phase are accompanied by a decrease in the radical concentration.

Thus, the introduction of ZnTPP into PHB led to condensation of the amorphous phase of the polymer during the fiber spinning process and, accordingly, to deceleration of the molecular mobility. The proportion of dense domains increased and, as a result, the radical concentration in the fiber decreased.

Next, we studied nonwoven fibrous materials containing the Fe(III)ClTPP complex. As seen from Fig. 5, addition of this complex to the PHB solution caused significant changes in the fiber morphology. The original PHB fiber (Fig. 1a) exhibited alternation of cylindrical and spindle-like segments. The presence of thickened segments in the fiber structure can be explained by low electrical conductivity and low surface tension of the polymer spinning solution. The average diameter of the cylindrical segments of the fiber was estimated at 1–6 μm, and the spindle-like segments had a maximum diameter of ~10 μm and a length of 20–30 μm. Adding 1% Fe(III)ClTPP complex led to the formation of

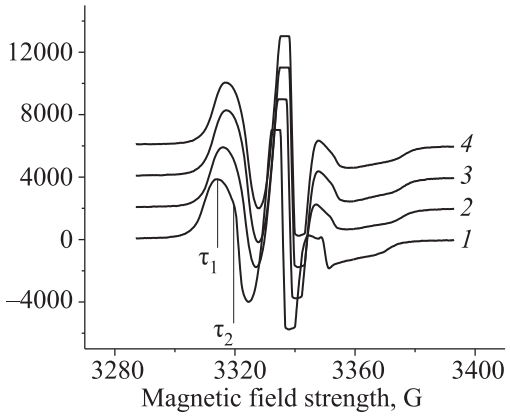

Fig. 4. ESR spectra of TEMPO nitroxyl radical in the PHB+ZnTPP samples containing (*1*) 0, (*2*) 1, (*3*) 3, and (*4*) 5% ZnTPP; (τ_1) fast and (τ_2) slow component.

fibers with average diameters of 1.5, 3, and 5 μm in the fibrous material. Fibers formed at higher Fe(III)ClTPP concentrations had an average diameter of 3 μm, while fibers with diameters of 1.5 and 6 μm almost completely disappeared (Fig. 5b).

DSC studies of the fibrous materials revealed a sharp increase in the proportion of the crystalline phase of PHB with increasing FeClTPP concentration in the mixed composition. The data obtained suggest that porphyrin produced a plasticizing effect on the PHB crystallization in the fiber electrospinning process. Specifically, the addition of FeClTPP caused increases in the intermolecular distance and the mobility of the chain. This facilitated orientation with increasing FeClTPP concentration, leading to increased proportion of crystallites and mesomorphic structures.

The data from small-angle X-ray diffraction analysis of the original PHB fibers and of the PHB fibers of different compositions, containing FeClTPP drug, suggest the following. Adding FeClTPP caused an increase in the proportion of interfibrillar regions with high proportions of oriented macromolecules, and specifically these

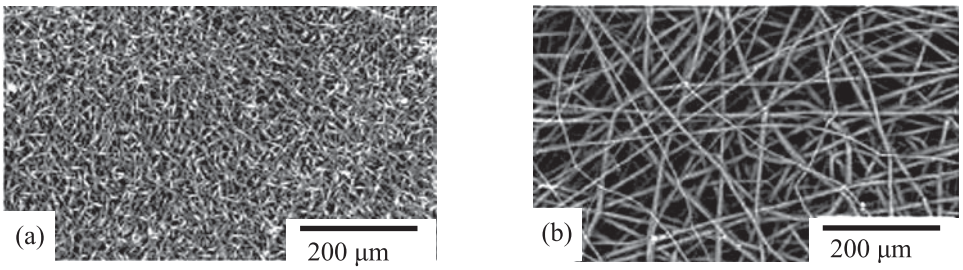

Fig. 5. SEM micrographs of (a) PHB and (b) PHB+3%Fe(III)ClTPP fibrous materials.

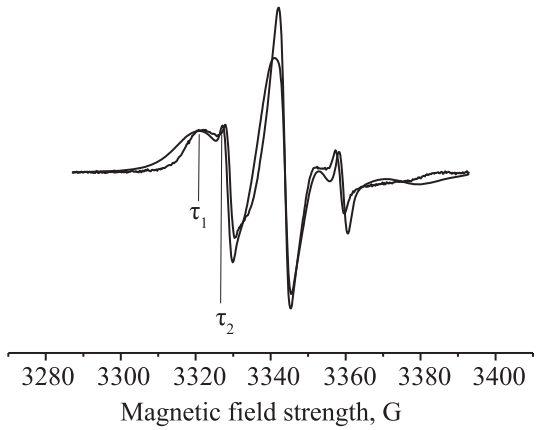

Fig. 6. Experimental ESR spectra of TEMPO nitroxyl radical for the PHB+3% FeClTPP fibers: (τ_1) fast and (τ_2) slow component.

molecules produced additional crystalline formations with a higher longitudinal size.

The structure of the amorphous domains is largely determined by the proportion of crystalline formations. Accordingly, adding low FeClTPP concentrations caused an increase in the degree of crystallinity of PHB and a change in the crystallite sizes, thereby affecting the structural and dynamic properties of the amorphous domains.

As seen from the ESR data (Fig. 6), an increase in the FeClTPP concentration in the fiber caused the proportion of dense domains to increase. The same holds to the radical correlation time, whereby the molecular mobility decelerated in the dense domains of the polymer, while remained practically unchanged in the loose domains of the amorphous phase.

Data from experiments on inoculation of test cultures [*S. aureus* p 209 (*Staphylococcus aureus*), *S. typhimurium* (*Salmonella typhimurium*), and *E. coli 1257 (Escherichia coli*)] on the PHB-based nonwovens impregnated with iron(III) porphyrin complex are indicative of good prospects for hygienic application of these materials [14].

CONCLUSIONS

Based on the experimental data obtained in this study, all the samples of the nonwoven material prepared from PHB by the electrospinning method at the process parameters maintained in the range specified can be divided into three groups that reliably describe the properties of the material structure: those characterized by regular, medium, and random fiber distribution. The mutual influence of the crystalline and amorphous domains in crystallizing biopolymers and their compositions remains a fairly complex and poorly studied area of modern polymer materials science. Our research showed that adding low ZnTPP concentrations to the PHB fibers caused an increase in the proportion of crystalline and paracrystalline structures. As a response to these changes in the crystalline phase, changes in the spin probe rotation dynamics in the amorphous domains were observed. X-ray diffraction analysis showed that 1–5% ZnTPP additions caused no changes in the supramolecular structure of PHB, including the unit cell parameters of the crystal structure, degree of crystallinity, crystallite size, long period, and degree of crystallinity in the fibril. At the same time, adding Fe(III)ClTPP led to additional crystallization and condensation of the amorphous domains in the PHB fibers.

Biochemical tests revealed a great potential offered by the PHB-based nonwoven fibrous materials for medical applications, e.g., for treatment of skin bacterial diseases. Our experiments confirmed the effectiveness of ozone sterilization of products based on these materials without compromising their mechanical properties.

FUNDING

This study was carried out with the use of equipment of the "New Materials and Technologies" Collective Use Center, Emanuel Institute of Biochemical Physics, Russian Academy of Sciences. The DSC analyses were conducted at the Semenov Institute of Chemical Physics, Russian Academy of Sciences, within the framework of theme no. AAAA-A17-117040610309-0.

CONFLICT OF INTEREST

No conflict of interest was declared by the authors.

REFERENCES

1. Malakhov, S.N. and Chvalun, S.N., *Russ. J. Gen. Chem*., 2017, vol. 87, no. 6, pp. 1364–1379. https://doi.org/10.1134/S107036321706038X
2. Olkhov, A.A., Tyubaeva, P.M., Staroverova, O.V., Mastalygina, E.E., Popov, A.A., Ischenko, A.A., and Iordanskii, A.L., *AIP Conf. Proc*., 2016, vol. 1736. https://doi.org/ 10.1063/1.4949673
3. Ol'khov, A.A., Tyubayeva, P.M., Lobanov, A.V., Mokerov, O.A, Karpova, S.G., and Iordanskii, A.L., *Vestn. Tekhnol. Univ*., 2017, vol. 20, no. 17, p. 5–12.
4. Shtil'man, M.I., *Tekhnologiya polucheniya polimerov mediko-biologicheskogo naznacheniya* (Technology of Preparation of Polymers for Biomedical Purposes),

Moscow: Akademkniga, 2006, p. 312.

5. Schiffman, J.D. and Schauer, C.A., *Polym. Rev*., 2008, vol. 48, no. 2, pp. 317–352. https://doi.org/10.1080/15583720802022182
6. Xie, G., Wang, Y., Han, X., Gong, Y., Wang, J., Zhang, J., Deng, D., and Liu, Y., *Ind. Eng. Chem. Res*., 2016, vol. 55, no. 26, p. 7116. https://doi.org/10.1021/acs.iecr.6b00958
7. Solov'eva, A.B., Belyaev, V.E., Glagolev, N.N., Volkov, V.I., Luzgina, B.N., Vstovskii, G.V., and Timashev, S.F., *Russ. J. Phys. Chem. A*, 2005, vol. 79, no. 4, pp. 635–644.
8. Kong, L. and Ziegler, G.R., *Biomacromolecules*, 2012, vol. 13, p. 2247. https://doi.org/10.1021/bm300396j
9. Zharkova, I.I., Staroverova, O.V., Voinova, V.V., Andreeva, N.V., Shushkevich, A.M., Sklyanchuk, E.D., Kuz'micheva, G.M., Bespalova, A.E., Akulina, E.A., Shaitan, K.V., and Ol'khov, A.A., *Biomed. Khim*., 2014, vol. 60, no. 5, p. 553.
10. Karpova, S.G., Ol'khov, A.A., Iordanskii, A.L., Lomakin, S.M., Shilkina, N.S., and Popov, A.A., *Russ. J. Phys. Chem. B*., 2016, vol. 10, p. 687. https://doi.org/10.1134/S1990793116040230
11. Lobanov, A.V., Nevrova, O.V., Ilatovskii, V.A., Sin'ko, G.V., and Komissarov, G.G., *Makrogeterotsikly*, 2011, vol. 4, no. 2, pp. 132–134.
12. Alopina, E.V., Usacheva, T.S., Ageeva, T.A., and Koifman, O.I., *Russ. J. Gen. Chem*., 2017, vol. 87, no. 12, pp. 3097–3101. https://doi.org/10.1134/S1070363217120593
13. Pechnikova, N.L., Ageeva, T.A., and Syrbu, S.A., *Russ. J. Gen. Chem*., 2017, vol. 87, no. 12, p. 3102. https://doi.org/10.1134/S107036321712060X
14. Kononenko, A.B., Bannikova, D.A., Savinova, E.P., Ol'khov, A.A., and Lobanov, A.V., *Probl. Veter. Sanit. Gig. Ekol*., 2017, no. 4, pp. 83–88.